Electrochemistry Communications 60 (2015) 153–157

Contents lists available at ScienceDirect

Electrochemistry Communications

journal homepage: www.elsevier.com/locate/elecom

Controlled preparation of carbon nanotube-conducting polymer composites at the polarisable organic/water interface

P.S. Toth *, A.K. Rabiu, R.A.W. Dryfe **

School of Chemistry, University of Manchester, Oxford Road, Manchester M13 9PL, UK

ARTICLE INFO

Article history:
Received 7 August 2015
Received in revised form 21 August 2015
Accepted 26 August 2015
Available online 3 September 2015

Keywords:
Interfacial polymerisation
Carbon nanotube film
Nanocomposite

ABSTRACT

The electro-polymerisation of polypyrrole (PPy) at the interface between two immiscible electrolyte solutions (ITIES) is reported. The approach is used to demonstrate the formation of a carbon nanotube (SWCNT)-conducting polymer composite, by performing polymerisation in the presence of an assembly of SWCNT films. The morphology of the SWCNT/PPy nanocomposites was determined using probe and electron microscopy and complementary spectroscopic techniques (EDAX, Raman).

© 2015 The Authors. Published by Elsevier B.V. This is an open access article under the CC BY license (http://creativecommons.org/licenses/by/4.0/).

1. Introduction

Intrinsically conducting polymers (CPs) have been the focus of great interest in many areas of science and technology during the last decades due to the attractive properties of these materials, *i.e.* the redox transformation can be used to induce conductance, spectral, mass, and volume changes [1,2]. These externally switchable changes are the basis of important applications of CPs such as electronic devices, sensors, smart windows, artificial muscles, and as membranes or modified electrodes [3–7]. The mechanical, thermal and electronic properties of CPs can be greatly enhanced by the formation of CP-carbon nanotube (CNT) composite materials: key factors are the method of preparation of the composite material, which in many cases can impart an useful anisotropic component to the physical properties of the composite [8,9]. One method of achieving such anisotropy is to grow the polymer materials around the aligned CNT "forest", where the latter is prepared *via* chemical vapour deposition (CVD) [10]. It has been shown that polymerisation can be advantageously achieved through electrochemical methods, where the CNT is used as the working electrode to produce an intimate contact between the carbon nanostructure and the polymeric deposit [4,6]. Single wall carbon nanotubes (SWCNTs) or their composites with CPs and metal nanoparticles can be characterised through Raman spectroscopy [11–14]. The most significant Raman bands of SWCNTs are the radial breathing mode (*RBM*), the tangential displacement mode (*TG*), which is also known as the *G* band, the disorder induced mode, which shows the density of the defects (*D*), and the high-frequency two-phonon mode (*2D* or *G′*) [15].

There has been a recent upsurge in reports on the *in situ* assembly/deposition of nanostructured materials (*e.g.* photoactive oxides, metallic nanostructures, and low-dimensional carbon species, such as SWCNTs and graphene (GR)) at the interface between two immiscible electrolyte solutions (ITIES) [16–20]. The ITIES is a special case of the generic liquid/liquid interface, where the presence of electrolyte in both phases provides external control over charge transfer, specifically ion, electron, and proton-coupled electron transfers [21–23]. Electropolymerisation at the ITIES has been reported: work on 2,2′:5′,2″-terthiophene [24], was followed by studies of the influence of different polymerisation conditions and characterisation of this low oxidation potential thiophene derivative [25,26], and pyrrole derivatives (1-methylpyrrole and 1-phenylpyrrole) [27]. The interfacial polymerisation of polypyrrole (PPy) and polyaniline (PANI) at the non-polarised, chloroform/water interface using ferric chloride ($FeCl_3$) as oxidant was reported in 2008 [28], and thereafter several papers described preparation of CPs at the liquid/liquid interface [29–33]. Numerous studies have also reported the formation of adsorbed carbon nanomaterial films *via* self-assembly, such as CNTs, and adsorbed films of few-layer GR or reduced graphene-oxide (rGO) at non-polarised, liquid/liquid interfaces, often with the specific aim of preparing transparent or modified carbon-coated electrode materials [34–37]. Recently we have extended this approach to the localisation and moreover the functionalisation of CVD GR at the ITIES [38,39]. The Zarbin group have demonstrated interfacial polymerisation using CNT or GR assembled at the non-polarised water/toluene interface to prepare carbon nanomaterial–PANI composites [40–42], mainly using a chemical oxidising agent, *i.e.* ammonium persulfate. The main advantages of the electro-polymerisation procedures, compared to the chemical route,

* Corresponding author. Tel.: +44 161 306 2770; fax: +44 161 275 4598.
** Corresponding author. Tel.: +44 161 306 4522; fax: +44 161 275 4598.
E-mail addresses: peter.toth@manchester.ac.uk (P.S. Toth), robert.dryfe@manchester.ac.uk (R.A.W. Dryfe).

http://dx.doi.org/10.1016/j.elecom.2015.08.022
1388-2481/© 2015 The Authors. Published by Elsevier B.V. This is an open access article under the CC BY license (http://creativecommons.org/licenses/by/4.0/).

consist of the possibility to control: the nucleation rate and growth by selecting the electro-polymerisation parameters; the thickness of the polymer films by the amount of charge passed during the deposition; and the CPs' morphology using suitable selection of an appropriate solvent and supporting electrolyte [7].

In this communication we report the interfacial electropolymerisation process for the controlled, potentiodynamic preparation of PPy films either at the bare ITIES or on the SWCNTs assembled interface. These free-standing PPy and SWCNT/PPy composite layers are transferable to solid substrates: these functional coatings are characterised using various microscopic and spectroscopic techniques.

2. Material and methods

Lithium chloride (LiCl, 99%); ammonium hexachloroiridate (IV) ($(NH_4)_2IrCl_6$, 99.99%); ammonium hexachloroiridate (III) monohydrate ($(NH_4)_3IrCl_6$, 99.99%); and the organic solvent 1,2-dichlorobenzene (DCB, 99%) were used as received, the pyrrole monomer (98%) was freshly distilled. The organic phase electrolyte bis(triphenylphosphoranylidene) tetrakis(pentafluorophenyl) borate (BTPPATPFB) was prepared as described elsewhere [43]. The potassium salt, KTPFB was obtained from Alfa Aesar, and the other chemicals were purchased from Sigma-Aldrich. Deionised water (18.2 MΩ cm resistivity), purified by a "PURELAB" Ultrafiltration unit (Elga Process Water), and was used for aqueous solution preparation.

Electrochemical experiments were performed using a four-electrode configuration [44] with an Autolab PGSTAT100 potentiostat (Metrohm-Autolab). The Galvani potential scale ($\Delta_o^w \Phi$) was normalised in every case using the formal transfer potential of tetramethylammonium cation, which corresponds to $\Delta_o^w \Phi^\circ = 0.277$ V [45]. The assembly of SWCNTs (synthesised by an arc discharge method, Sigma-Aldrich) at the organic/water interface is described elsewhere [44]. Briefly, sonication for 12 h using an ultrasonic bath (Elmasonic P60H) operating at 37 kHz, at 30% of its full power was used to prepare the SWCNT dispersion in DCB, the temperature was kept below 30 °C with a recirculating cooler system (Julabo F250) attached to the ultrasonic bath. Then, an aliquot of the dispersion with the organic electrolyte solution in DCB and an equal volume of aqueous phase were placed in contact and self-assembly of the SWCNT was induced using sonication (15 min). UV–Vis spectroscopy (DH-2000-BAL, Ocean Optics and USB2000 interface, Micropack GmbH) was used to measure the concentration of the SWCNT dispersions. Raman analysis (Renishaw RM 264 N94 (532 nm laser) spectrometer operating at power ≤ 0.3 mW), the SEM (Philips XL30 ESEM-FEG, operated at 10 kV) and the AFM (Bruker MultiMode 8, operated in "Peak Force" tapping mode with a silicon tip on a silicon nitride lever) characterisations were performed on the samples once transferred to a Si/SiO_2 wafer, following interfacial polymerisation, either for the PPy films or the SWCNT/PPy composite layers. The displayed errors are based on standard deviations from arithmetic averages of multiple measured values.

3. Results and discussion

3.1. Dynamic electro-polymerisation of PPy at ITIES

The successful interfacial electro-polymerisation of PPy film was achieved by a simple redox reaction between pyrrole (Py) oxidation to PPy (on the organic side of interface) and aqueous phase hexachloroiridate (IV) ($IrCl_6^{2-}$), which is reduced to hexachloroiridate (III) ($IrCl_6^{3-}$, Reaction 1).

$$IrCl_6{}^{2-}(aq) + Py(o) \rightarrow IrCl_6{}^{3-}(aq) + PPy(s) + H^+(aq) \quad (1)$$

The PPy films were prepared using dynamic electro-polymerisation, either *via* cyclic voltammetry at a 100 mV s^{-1} scan rate or by potential step, from 0.1 M pyrrole (organic (o), DCB phase) and aqueous (aq) phase containing 1 mM $IrCl_6^{2-}$ and 0.1 mM $IrCl_6^{3-}$ (composition of the cells given in Fig. 1). BTPPATPFB (10 mM) and LiCl (0.1 M) were used as (o) and (aq) phase supporting electrolytes, respectively. Four different dynamic interfacial polymerisation protocols were used: cyclic voltammograms (CVs) with 25 (Fig. 1A), 50 (Fig. 2B), 75 (Fig. 1B) cycles and the potential step method. The difference in the PPy films' and the blank CV's (blank = no pyrrole, Fig. 1 cell 1) electro-activity can be observed by comparing the last CVs of each polymerisation, *i.e.* the 25th (Fig. 1A-b) and 75th (Fig. 1B-b) cycles (Fig. 1 cell 2).

The main features of the PPy Raman spectra were assigned according to the literature [46] as follows (Fig. 1C, marked by asterisks): the ring deformation (933 cm^{-1}), the C—H in plane bending (984 cm^{-1}), the C—C backbone stretching (1318 cm^{-1}), the C═C backbone stretching (1562 cm^{-1}) vibration modes for the neutral form; and the C—H in-plane bending (1048 cm^{-1}), N—H in-plane bending (1254 cm^{-1}), C—C backbone stretching (1333–1415 cm^{-1}), C═C backbone stretching (1587–1587 cm^{-1}) for the cationic form, respectively, as the PPy films were partially doped both forms are present. In every case the transferred PPy films were shown to exhibit continuous coverage on the Si/SiO_2 substrate with the naked eye. The series of the SEM images of the transferred PPy films on Si/SiO_2 (Fig. 1D–F) show a trend in the extent of the coverage as a function of the number of the CV cycles, which were used for the electro-polymerisation of the PPy. Comparing the polymer films deposited using 25 (Fig. 1D), 50 (Fig. 1E), and 75 (Fig. 1F) cycles, the increase in coverage can be observed and moreover, a difference also can be seen in the morphology of the different PPy films. The initial deposits are globular, and consist of more discrete particles, whereas with further cycling the structure becomes more coherent, *i.e.* the PPy film in Fig. 1F is built up from flakes/layers, while applying the potential step method, more globular structure achieved.

3.2. Preparation of SWCNT/PPy composite at DCB/water interface

A schematic of the redox process and CVs of the electropolymerisation of PPy on the interfacial SWCNT film are shown in Fig. 2. During the reduction of the $IrCl_6^{2-}$ to $IrCl_6^{3-}$ on the aqueous side of the interface, the oxidation of the pyrrole occurred through the assembled SWCNT film at the interface, by analogy with similar redox reactions at the SWCNT assembled ITIES, *e.g.* Pd electrodeposition [44]. The optimised potentiodynamic polymerisation was used for the preparation of the single wall carbon nanotubes-based polypyrrole composite (hereafter, SWCNT/PPy), employing 50 CV cycles at a scan rate of 100 mV s^{-1}. The CV responses with and without the Py monomer are shown in Fig. 2B. The resultant SEM, AFM micrographs and Raman spectra of SWCNT/PPy and the comparison of the pristine (C) and PPy functionalised SWCNTs (F) are given in Fig. 2. The pristine SWCNTs formed bundles either on transfer to solid substrate or due to the presence of BTPPATPFB electrolyte (Fig. 2C), while in the case of the SWCNT/PPy, thinner or more individualised nanotubes are embedded in the PPy matrix (Fig. 2F), which can form a proper coating on the Si/SiO_2. This suggests that the drying process, rather than the removal of the electrolyte, is the cause of the bundling evident in Fig. 2C.

The AFM image of the composite (Fig. 2E) was used to estimate the thickness of the transferred SWCNT/PPy layer, found to be 31.8 ± 0.3 nm. The diameter of the nanotubes in the case of the pristine SWCNT was 6.2 ± 3.4 nm and the SWCNT/PPy was estimated to be in the range between 9.6 ± 0.5 nm to 14.9 ± 1.6 nm. The difference is attributed to the PPy "coating" deposited around the nanotubes between the pristine SWCNT and the composite ones. Fig. 2D-a and Fig. 2D-b, respectively, show the *RBM*, the two main components of the *G* band (G^- and G^+), and the *2D* band in Raman spectra of pristine SWCNT and SWCNT/PPy. The left inset in Fig. 2D presents the pristine (black) and composite (red) SWCNTs' spectra, due to the overlap of the *D* and *G* bands of the SWCNT and the significant peaks of the PPy, it is hard to detect all of the polymer peaks. Nevertheless, the ring deformation

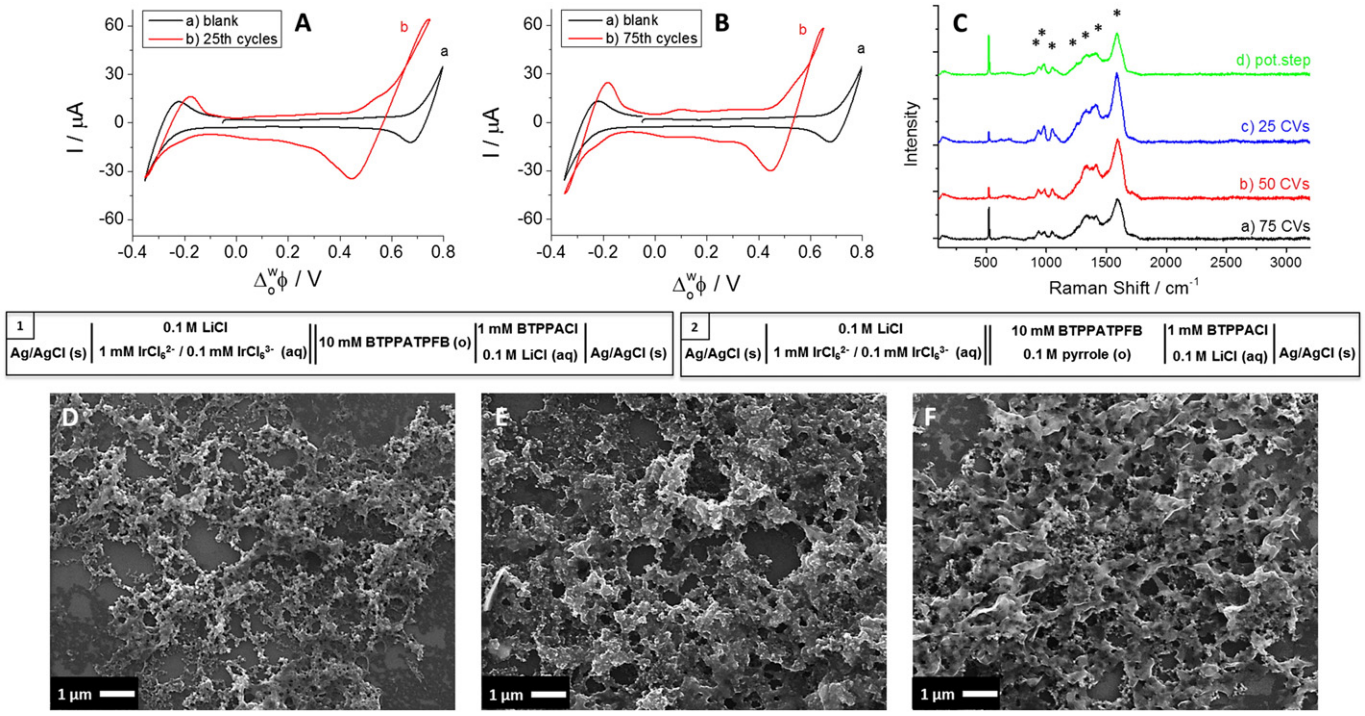

Fig. 1. A–B: Voltammetric responses of Cell 1 (trace a) and Cell 2 (trace b) at the DCB/water interface. C: Raman spectra (532 nm excitation laser) of the PPy films, prepared by different dynamic depositions: 75 CVs (a), 50 CVs (b), 25 CVs (c) at 100 mV s^{-1} scan rate and using potential step method (d), the Raman bands associated with the PPy are marked by asterisks. The cell compositions for the blank (1) and for the dynamic polymerisation (2) are given along with SEM images of the transferred PPy films on Si/SiO_2, using 25 CVs (D), 50 CVs (E), and 75 CVs (F).

(942–1005 cm^{-1}), the C—H in-plane bending (1080–1121 cm^{-1}), and the C—C backbone stretching (1243–1275 cm^{-1}) vibrational modes for the neutral form, marked by asterisks, can be observed. There is a small up-shift of the nanotube *TG* mode mainly the G^- part, the band at around 1569 cm^{-1} in pristine SWCNT (black curve) is up-shifted to 1572 cm^{-1} in the SWCNT/PPy (red curve), as charge transfer occurs

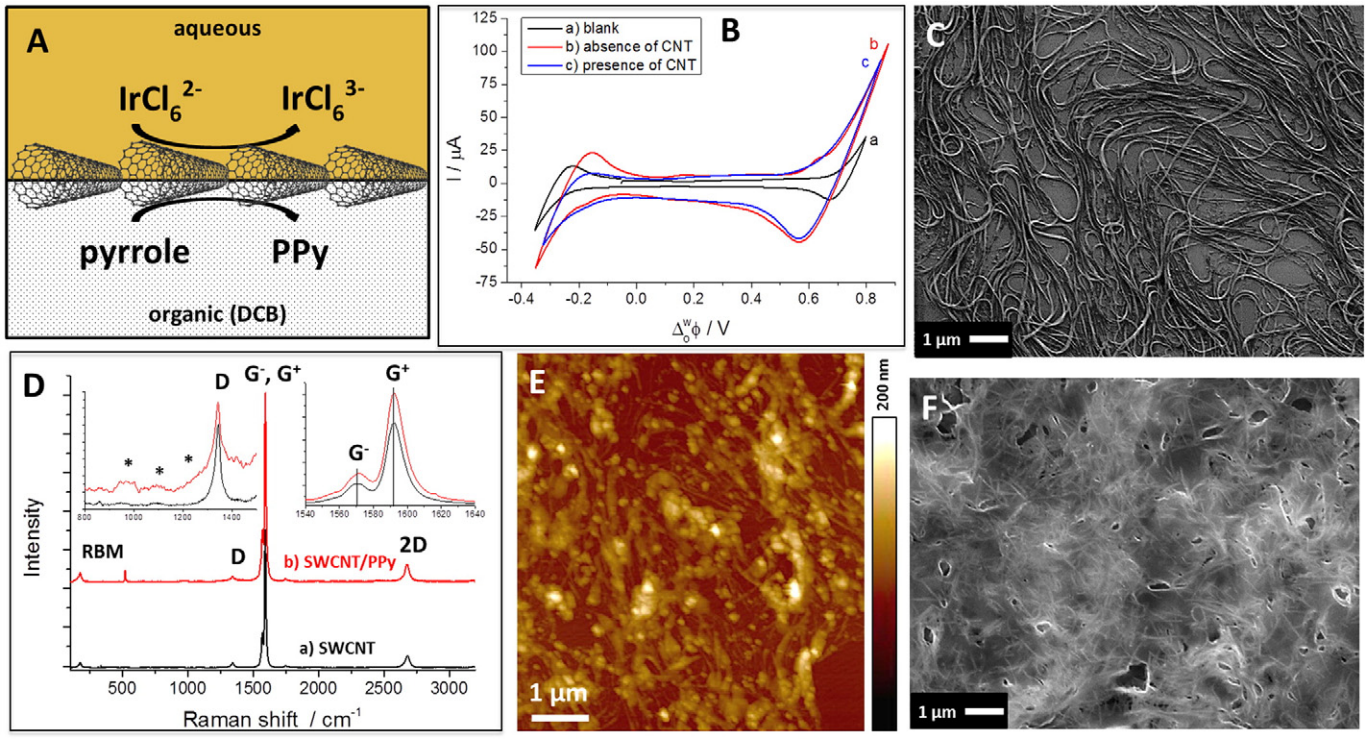

Fig. 2. A: Schematic of the assembled SWCNTs layer and the electro-polymerisation at the ITIES. B: CVs of interfacial pyrrole oxidation and reduction of $IrCl_6^{2-}$ in the absence (trace b) and in the presence of SWCNT film (trace c). For comparison, a "blank" CV without Py is shown (trace a), scan rate: 100 mV s^{-1}. The coverage of SWCNT at the DCB/water interface was 8.67 μg cm^{-2} in the case of B. SEM (C), Raman spectra (D), AFM (E) and further SEM (F) of the pristine SWCNTs (C, D-a) and the SWCNT/PPy composite material (D-b, E, F). Raman spectra (532 nm excitation laser) of the *D* band region (left inset of D) and the G^- and G^+ bands region (right inset of D). The SWCNT/PPy composite was prepared by 50 CV cycles at 100 mV s^{-1} scan rate.

from the PPy chains to the SWCNT due to balancing of the redox potentials of both species (right inset in Fig. 2D) [11], causing the partial doping of SWCNT in the composite. The properties of the carbon nanotubes/conducting polymer composites would be dependent on the semiconducting or metallic type of SWCNT and on the nature of the conducting polymer used [11,47]. Thus, by selecting an appropriate type of SWCNT and conducting polymer it is possible to tune the properties of the resultant composites. The *in situ* electrochemical methods for functionalizing nanoscale carbonaceous materials with CPs offer the alternative possibilities to control the structural properties of deposited polymer and the composite material.

4. Conclusion

The electro-oxidation of the pyrrole monomer was achieved at the bare and SWCNT assembled DCB/water interface. Different dynamic electro-polymerisation methods showed different morphology of the PPy layers, and an increase in the number of the voltammograms for the polymer films growth gave a better coverage after transfer to the solid substrate.

Carbon nanotube-based PPy nanocomposites were obtained using the optimised polymerisation, and the evidence of formation of the SWCNT/PPy layer was derived from its transfer to solid substrates and subsequent microscopic and spectroscopic analysis. The resultant SWCNT/PPy composite structure shows that the CNTs were embedded in the PPy matrix, in other words the PPy was polymerised around the SWCNTs. Moreover the changes in the intensity and position of the Raman *D* and *G* bands of the SWCNTs indicated a partial doping of the nanotubes, caused by the formation of the composite.

The applied dynamic preparation of SWCNT/PPY at ITIES allows for PPy to grow uniformly on the surface of SWCNTs and is suited for the preparation of free-standing conductive and continuous SWCNT/PPy films, which are immediately transferable, compared to the traditional electro-polymerisation procedures using carbon nanotube networks grown or assembled at solid substrates (*e.g.* vertically aligned CNT "forest").

This electro-polymerisation method, using the low-dimensional carbon materials assembled at the ITIES, represents a new approach for the preparation of carbon-nanomaterial/CP composites, which could be extended to production of metal NP/CP composites, using metal precursors in the aqueous phase. Fabrication of novel and modified, functional electrodes is possible by transferring these composite layers to a solid substrate.

Conflict of interest

The authors declare no competing financial interest.

Acknowledgement

The authors thank the U.K. EPSRC (EP/K007033/1) for financial support. A.K.R. thanks the Educational Trust Fund (Nigeria) for a PhD scholarship.

References

[1] H. Shirakawa, E.J. Louis, A.G. MacDiarmid, C.K. Chiang, A.J. Heeger, Synthesis of electrically conducting organic polymers: halogen derivatives of polyacetylene, (CH), J. Chem. Soc. Chem. Commun. (1977) 578–580.
[2] C. Janaky, G. Cseh, P.S. Toth, C. Visy, Application of classical and new, direct analytical methods for the elucidation of ion movements during the redox transformation of polypyrrole, J. Solid State Electrochem. 14 (2010) 1967–1973.
[3] B. Adhikari, S. Majumdar, Polymers in sensor applications, Prog. Polym. Sci. 29 (2004) 699–766.
[4] C. Janaky, C. Visy, Conducting polymer-based hybrid assemblies for electrochemical sensing: a materials science perspective, Anal. Bioanal. Chem. 405 (2013) 3489–3511.
[5] E. Peintler-Krivan, P.S. Toth, C. Visy, Combination of in situ UV–Vis-NIR spectroelectrochemical and a.c. impedance measurements: a new, effective technique for studying the redox transformation of conducting electroactive materials, Electrochem. Commun. 11 (2009) 1947–1950.
[6] C. Janaky, K. Rajeshwar, The role of (photo)electrochemistry in the rational design of hybrid conducting polymer/semiconductor assemblies: from fundamental concepts to practical applications, Prog. Polym. Sci. 43 (2015) 96–135.
[7] P.S. Sharma, A. Pietrzyk-Le, F. D'Souza, W. Kutner, Electrochemically synthesized polymers in molecular imprinting for chemical sensing, Anal. Bioanal. Chem. 402 (2012) 3177–3204.
[8] S.B. Yang, B.-S. Kong, D.-H. Jung, Y.-K. Baek, C.-S. Han, S.-K. Oh, H.-T. Jung, Recent advances in hybrids of carbon nanotube network films and nanomaterials for their potential applications as transparent conducting films, Nanoscale 3 (2011) 1361–1373.
[9] Z. Niu, P. Luan, Q. Shao, H. Dong, J. Li, J. Chen, D. Zhao, L. Cai, W. Zhou, X. Chen, S. Xie, A "skeleton/skin" strategy for preparing ultrathin free-standing single-walled carbon nanotube/polyaniline films for high performance supercapacitor electrodes, Energy Environ. Sci. 5 (2012) 8726–8733.
[10] R.J. Allen, O. Ghita, B. Farmer, M. Beard, K.E. Evans, Mechanical testing and modelling of a vertically aligned carbon nanotube composite structure, Compos. Sci. Technol. 77 (2013) 1–7.
[11] M. Kalbac, L. Kavan, L. Dunsch, An in situ Raman spectroelectrochemical study of the controlled doping of semiconducting single walled carbon nanotubes in a conducting polymer matrix, Synth. Met. 159 (2009) 2245–2248.
[12] A. Colina, V. Ruiz, A. Heras, E. Ochoteco, E. Kauppinen, J. Lopez-Palacios, Low resolution Raman spectroelectrochemistry of single walled carbon nanotube electrodes, Electrochim. Acta 56 (2011) 1294–1299.
[13] C. Fernandez-Blanco, D. Ibanez, A. Colina, V. Ruiz, A. Heras, Spectroelectrochemical study of the electrosynthesis of Pt nanoparticles/poly(3,4-(ethylenedioxythiophene) composite, Electrochim. Acta 145 (2014) 139–147.
[14] L. Kavan, P. Rapta, L. Dunsch, In situ Raman and Vis-NIR spectroelectrochemistry at single-walled carbon nanotubes, Chem. Phys. Lett. 328 (2000) 363–368.
[15] A. Jorio, R. Saito, J.H. Hafner, C.M. Lieber, M. Hunter, T. McClure, G. Dresselhaus, M.S. Dresselhaus, Structural (n, m) determination of isolated single-wall carbon nanotubes by resonant Raman scattering, Phys. Rev. Lett. 86 (2001) 1118–1121.
[16] A.N.J. Rodgers, S.G. Booth, R.A.W. Dryfe, Particle deposition and catalysis at the interface between two immiscible electrolyte solutions (ITIES): a mini-review, Electrochem. Commun. 47 (2014) 17–20.
[17] R.A.W. Dryfe, A.O. Simm, B. Kralj, Electroless deposition of palladium at bare and templated liquid/liquid interfaces, J. Am. Chem. Soc. 125 (2003) 13014–13015.
[18] H. Jensen, D.J. Fermin, J.E. Moser, H.H. Girault, Organization and reactivity of nanoparticles at molecular interfaces. Part 1. Photoelectrochemical responses involving TiO(2) nanoparticles assembled at polarizable water vertical bar 1,2-dichloroethane junctions, J. Phys. Chem. B 106 (2002) 10908–10914.
[19] N. Eugster, H. Jensen, D.J. Fermin, H.H. Girault, Photoinduced electron transfer at liquid vertical bar liquid interfaces. Part VII. Correlation between self-organisation and structure of water-soluble photoactive species, J. Electroanal. Chem. 560 (2003) 143–149.
[20] I. Hatay, P.Y. Ge, H. Vrubel, X. Hu, H.H. Girault, Hydrogen evolution at polarised liquid/liquid interfaces catalyzed by molybdenum disulfide, Energy Environ. Sci. 4 (2011) 4246–4251.
[21] Z. Samec, Electrochemistry at the interface between two immiscible electrolyte solutions, Pure Appl. Chem. 76 (2004) 2147–2180.
[22] I. Hatay, B. Siu, F. Li, R. Partovi-Nia, H. Vrubel, X. Hu, M. Ersoz, H.H. Girault, Hydrogen evolution at liquid–liquid interfaces, Angew. Chem. Int. Ed. 48 (2009) 5139–5142.
[23] M.D. Scanlon, X.J. Bian, H. Vrubel, V. Amstutz, K. Schenk, X.L. Hu, B.H. Liu, H.H. Girault, Low-cost industrially available molybdenum boride and carbide as "platinum-like" catalysts for the hydrogen evolution reaction in biphasic liquid systems, Phys. Chem. Chem. Phys. 15 (2013) 2847–2857.
[24] K. Gorgy, F. Fusalba, U. Evans, K. Kontturi, V.J. Cunnane, Electropolymerization of 2,2 ′: 5′,2 ″ terthiophene at an electrified liquid–liquid interface, Synth. Met. 125 (2001) 365–373.
[25] U. Evans-Kennedy, J. Clohessy, V.J. Cunnane, Spectroelectrochemical study of 2,2′: 5′,2″-terthiophene polymerization at a liquid/liquid interface controlled by potential-determining ions, Macromolecules 37 (2004) 3630–3634.
[26] A.S. Sarac, U. Evans, M. Serantoni, J. Clohessy, V.J. Cunnane, Electrochemical and morphological study of the effect of polymerization conditions on poly (terthiophene), Surf. Coat. Technol. 182 (2004) 7–13.
[27] V.J. Cunnane, U. Evans, Formation of oligomers of methyl- and phenyl-pyrrole at an electrified liquid/liquid interface, Chem. Commun. 2163–2164 (1998).
[28] N. Nuraje, K. Su, N.-l. Yang, H. Matsui, Liquid/liquid interfacial polymerization to grow single crystalline nanoneedles of various conducting polymers, ACS Nano 2 (2008) 502–506.
[29] M. Shen, Y. Han, X. Lin, B. Ding, L. Zhang, X. Zhang, Preparation and electrochemical performances of porous polypyrrole film by interfacial polymerization, J. Appl. Polym. Sci. 127 (2013) 2938–2944.
[30] S. Harish, J. Mathiyarasu, K.L.N. Phani, Generation of gold–PEDOT nanostructures at an interface between two immiscible solvents, Mater. Res. Bull. 44 (2009) 1828–1833.
[31] M. Gniadek, S. Malinowska, T. Rapecki, Z. Stojek, M. Donten, Synthesis of polymer–metal nanocomposites at liquid–liquid interface supported by ultrasonic irradiation, Synth. Met. 187 (2014) 193–200.
[32] B. Anothumakkool, R. Soni, S.N. Bhange, S. Kurungot, Novel scalable synthesis of highly conducting and robust PEDOT paper for a high performance flexible solid supercapacitor, Energy Environ. Sci. 8 (2015) 1339–1347.
[33] C. Johans, J. Clohessy, S. Fantini, K. Kontturi, V.J. Cunnane, Electrosynthesis of polyphenylpyrrole coated silver particles at a liquid–liquid interface, Electrochem. Commun. 4 (2002) 227–230.

[34] R.V. Salvatierra, S.H. Domingues, M.M. Oliveira, A.J.G. Zarbin, Tri-layer graphene films produced by mechanochemical exfoliation of graphite, Carbon 57 (2013) 410–415.
[35] S. Gan, L. Zhong, T. Wu, D. Han, J. Zhang, J. Ulstrup, Q. Chi, L. Niu, Spontaneous and fast growth of large-area graphene nanofilms facilitated by oil/water interfaces, Adv. Mater. 24 (2012) 3958–3964.
[36] Z. Tang, J. Zhuang, X. Wang, Exfoliation of graphene from graphite and their self-assembly at the oil–water interface, Langmuir 26 (2010) 9045–9049.
[37] K. Bramhaiah, N.S. John, Hybrid films of reduced graphene oxide with noble metal nanoparticles generated at a liquid/liquid interface for applications in catalysis, RSC Adv. 3 (2013) 7765–7773.
[38] P.S. Toth, Q.M. Ramasse, M. Velicky, R.A.W. Dryfe, Functionalization of graphene at the organic/water interface, Chem. Sci. 6 (2015) 1316–1323.
[39] P.S. Toth, M. Velicky, Q.M. Ramasse, D.M. Kepaptsoglou, R.A.W. Dryfe, Symmetric and asymmetric decoration of graphene: bimetal–graphene sandwiches, Adv. Funct. Mater. 25 (2015) 2899–2909.
[40] R.V. Salvatierra, M.M. Oliveira, A.J.G. Zarbin, One-pot synthesis and processing of transparent, conducting, and freestanding carbon nanotubes/polyaniline composite films, Chem. Mater. 22 (2010) 5222–5234.
[41] S.H. Domingues, R.V. Salvatierra, M.M. Oliveirab, A.J.G. Zarbin, Transparent and conductive thin films of graphene/polyaniline nanocomposites prepared through interfacial polymerization, Chem. Commun. 47 (2011) 2592–2594.
[42] V.H. Rodrigues de Souza, M.M. Oliveira, A.J.G. Zarbin, Thin and flexible all-solid supercapacitor prepared from novel single wall carbon nanotubes/polyaniline thin films obtained in liquid–liquid interfaces, J. Power Sources 260 (2014) 34–42.
[43] B. Su, J.-P. Abid, D.J. Fermín, H.H. Girault, H. Hoffmannová, P. Krtil, Z. Samec, Reversible voltage-induced assembly of Au nanoparticles at liquid|liquid interfaces, J. Am. Chem. Soc. 126 (2004) 915–919.
[44] P.S. Toth, A.N.J. Rodgers, A.K. Rabiu, R.A.W. Dryfe, Electrochemical activity and metal deposition using few-layer graphene and carbon nanotubes assembled at the liquid–liquid interface, Electrochem. Commun. 50 (2015) 6–10.
[45] B. Hundhammer, C. Muller, T. Solomon, H. Alemu, H. Hassen, Ion transfer across the water–o-dichlorobenzene interface, J. Electroanal. Chem. 319 (1991) 125–135.
[46] A. Kepas, M. Grzeszczuk, C. Kvarnstrom, T. Lindfors, A. Ivaska, UV–Vis and Raman spectroelectrochemistry of electrodeposited polypyrrole in hexafluorophosphate, Pol. J. Chem. 81 (2007) 2207–2214.
[47] M. Kalbac, L. Kavan, M. Zukalova, L. Dunsch, An in situ Raman spectro-electrochemical study of the controlled doping of single walled carbon nanotubes in a conducting polymer matrix, Carbon 45 (2007) 1463–1470.